

Article

Nature-Inspired Frequency Selective Surface in Fibonacci Spiral with Closely Resonant Bands

Maciel Alves de Oliveira¹ , Pavlos I. Lazaridis² , Zaharias D. Zaharis³ , Alfredo Gomes Neto⁴ ,
Antônio L. P. S. Campos⁵ , Alexandre J. R. Serres¹ 

¹Department of Electrical Engineering, Federal University of Campina Grande (UFCG), Campina Grande, Brazil, maciel.oliveira@ee.ufcg.edu.br, alexandreserres@dee.ufcg.edu.br

²School of Computing and Engineering, University of Huddersfield, Huddersfield, U.K, P.Lazaridis@hud.ac.uk

³Department of Electrical and Computer Engineering, Aristotle University of Thessaloniki, Thessaloniki, Greece, zaharis@auth.gr

⁴Federal Institute of Education, Science and Technology of Paraíba (IFPB), Campus João Pessoa, Paraíba, Brazil, alfredogomesjpa@gmail.com

⁵Communication Engineering Department, Federal University of Rio Grande do Norte (UFRN), Natal, Brazil, alpscampos@gmail.com

Abstract— This paper presents a novel nature-inspired tri-band frequency selective surface (FSS) characterized by closely spaced bands, angular stability, and polarization independence. The FSS element adopts a segmented Fibonacci spiral geometry. While a single-segmented Fibonacci spiral does not inherently possess polarization independence, the proposed proof of concept achieves this by cascading the same design geometry rotated by 90° between them. Resonant frequencies of 1.63 GHz, 2.46 GHz, and 3.43 GHz are achieved, with minimal separation ratios of 1.5 from the second to the first frequency and 1.4 from the third to the second. Additionally, angular stability is confirmed up to 45°. Simulation of the FSS is conducted using HFSS software, and the simulated results are rigorously validated against experimental data, demonstrating excellent agreement.

Index Terms— closely resonant bands, Fibonacci spiral, FSS, Nature-inspired.

I. INTRODUCTION

Frequency-selective surfaces (FSSs) have been investigated for decades due to numerous applications, including microwave, millimeter-wave, and Terahertz frequency spectra, ranging from more traditional applications in dual-band antenna systems, rockets, missiles, and antenna radomes [1], [2], to more recent applications such as radio frequency identification (RFID) [3], lenses [4], and protection against electromagnetic interference (EMI) [5].

Some of these applications may require closely spaced multiple resonance band responses. Two bands are considered close if the frequency ratio (FR) between their bands is less than an octave (< 2) [6]. Additionally, angular stability and polarization independence are other desired characteristics.

FSSs with traditional geometries may not exhibit these characteristics simultaneously. Over the years, various techniques have been developed to design an FSS with all these desired properties, including

cascade structures, fractal elements, convoluted elements, and combined elements [7] – [11]. In this context, exploring nature-inspired geometries for designing unit cells of FSSs can be of significant interest to scientific and technological development, offering the potential to enhance the characteristics of numerous devices and circuits used in high-frequency applications.

The term "nature-inspired" has been broadly defined as the utilization of analogous biological systems to develop solutions to engineering problems [12]. This definition can be extended to encompass non-biological natural systems, thereby encompassing nature-inspired design. As such, nature-inspired designs may not necessarily resemble their natural counterparts superficially or morphologically, but rather function or behave similarly. The exploration of nature-inspired geometries can yield structures with responses conducive to a wide range of applications, significantly contributing to the enhancement of FSS technology.

The paper presents the proof of concept that two Fibonacci spirals cascaded and rotated by 90° between them demonstrate polarization independence, whereas individually they exhibit dependence. The unit cell exhibits a tri-band response with closely resonant bands ($FR < 2$), angular stability, and polarization independence. The frequency ratio (FR) from the second to the first resonant frequencies is 1.48, and the FR from the third to the second resonant frequencies is 1.43. The proposed FSS features nulls that can be utilized in applications at ISM (2.40 to 2.4835 GHz) and 5G NR bands (3.3 to 3.7 GHz). These closely matched responses have been achieved due to the nature-inspired FSS structure. The cascaded FSS enables angular stability and polarization independence. Furthermore, the FSS is a low-cost and easy-to-fabricate structure.

II. STATE OF THE ART

Scientists and engineers draw inspiration from nature for both functional and commercial applications. Numerous species and objects found in nature exhibit patterns that adhere to the so-called golden ratio and Fibonacci numbers [13]–[15]. These proportions and patterns have the potential to enhance the performance of systems [16]. In recent years, there has been a growing interest among the telecommunications scientific community in designing electromagnetic devices based on biological or natural analogies.

In [17], a nature-inspired geometry is proposed for the development of an innovative FSS. The chosen shape for the unit cell geometry is based on the triangular leaf of the Oxalis plant, which features three axes of symmetry with leaves resembling triangles. Although the operating frequency is close to 3.5 GHz, polarization independence and angular stability are not demonstrated.

In [18], the authors analyzed a complementary FSS for electromagnetic shielding applications. The FSS element geometry is based on a closed Fibonacci spiral combined with a square loop. The complementary FSS achieved a multiband frequency response, with two stopbands at 6.5 GHz and 15.4 GHz and a transmit band at 9.85 GHz. The structure exhibited angular stability, although the authors did not demonstrate polarization independence.

Another study based on the Fibonacci spiral is presented in [19]. A double resonance is achieved through the combined effect of the square loop with the Fibonacci spiral. The same pattern is printed on both sides of the substrate and coupled with the aid of metallic pathways to form a 2.5D element. The proposed structure exhibits bandpass characteristics in the frequency range from 9.5 to 12.58 GHz. Additionally, the proposed FSS demonstrates angular stability up to 60° and polarization independence.

A geometry based on the Archimedes spiral is proposed in [20]. The FSS utilizes a four-armed spiral. Each arm terminates in a half-circle with a radius equal to half the arm's width, and a similar process is applied at the center of the spiral. The initial resonant frequency is 3.91 GHz, and with each layer added to the FSS superstrate, the resonant frequency decreases, reaching 2.94 GHz. However, the authors did not discuss either polarization independence or angular stability.

In [21], strategies are presented for designing an FSS with a dual-band frequency response, based on four- and eight-armed Archimedean spirals. The individual lengths of the spiral arms are utilized as an initial design parameter. However, the study did not investigate angular stability or polarization independence.

Segmented spiral elements as a geometry of unit cells for FSS design are presented in [22]. The FSS exhibits a multiband frequency response, operating within the 2 to 18 GHz range. The number and frequency of resonances are determined by the spiral geometry design. Additionally, the transmission spectrum is influenced by the tilt angle, rotation angle of the spiral, and the polarization of the receiving antenna. However, the structure did not demonstrate angular stability or polarization independence.

This work proposes a cascaded FSS with a segment of the Fibonacci spiral as an element of the unit cell. The cascaded FSSs utilize the same design geometry, rotated by 90° between them. The proposed cascaded FSSs are superior to other FSSs previously proposed in the literature because they offer a frequency response with multiple closely resonant bands along with angular stability and polarization independence. Table I presents a comparison between our work and recent studies found in the literature. The proposed FSS offers polarization independence and angular stability of up to 45 degrees. Furthermore, the structure is easy to manufacture, making it attractive in comparison of other works.

TABLE I. COMPARISON BETWEEN RECENT STUDIES AND OUR WORK

Work	Geometry	Polarization Independence	Angular Stability	Ease of Manufacturing
[17]	Triangular leaf of the Oxalis plant	–	Up to 30°	Medium
[18]	Closed Fibonacci spiral combined with a square loop	–	Up to 60°	Hard
[19]	Closed Fibonacci spiral combined with a square loop	Yes	Up to 60°	Hard
[20]	Archimedes spiral	–	–	Medium
[21]	Archimedes spiral	–	–	Medium
[22]	Segmented Fibonacci spiral	–	–	Medium
Our work	Segmented Fibonacci spiral	Yes	Up to 45°	Easy

III. PARAMETRIC ANALYSIS

In this work, we aim to advance the study of FSSs by exploring the use of nature-inspired geometries in developing FSSs with closely resonant bands, angular stability, and polarization independence. To achieve this, we consider a segmented Fibonacci spiral as the geometry of the unit cell. The Fibonacci spiral is a pattern widely observed in nature, with examples including nautilus shells (Fig. 1), which exemplify the Fibonacci sequence [23].



Fig. 1. Nautilus shell as an example of the Fibonacci spiral in nature [23].

The Fibonacci spiral can be generated from the polar equation as:

$$r = ae^{(b\theta)} \quad (1)$$

where r is the radius of each turn of the spiral, a and b are arbitrary constants depending on the specific spiral, and θ is the angle of rotation as the curve spirals [24]–[26]. In the work presented here, the cascaded FSS element draws inspiration from nature, specifically the Fibonacci spiral. For the design of the nature-inspired FSS, a fiberglass dielectric material, specifically FR4, is considered, with a relative permittivity of 4.4, a loss tangent of 0.02, and a thickness $h = 1.58$ mm.

The width of the spiral strip is $w = 0.3$ mm, while the periodicity is $P = 35$ mm. For this cell size, the constants a and b of the spiral are set equal to 1.8 and 0.155, respectively, with θ varying up to 5π . Fig. 2(a) and Fig. 2(b) illustrate the proposed geometry. These physical dimensions were determined through an extensive parametric analysis, involving over 200 simulations where parameters such as r , a , b , θ , and P were varied.

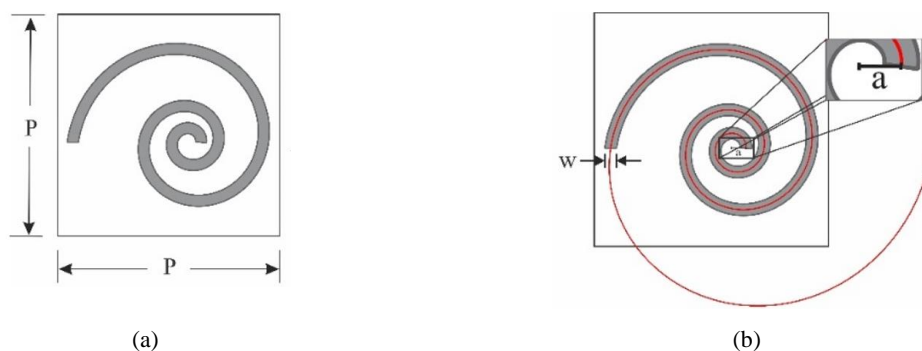


Fig. 2. Geometry of the unit cell: (a) periodicity and (b) details of the Fibonacci spiral.

All simulations were conducted using the commercial software Ansys Electronics Desktop with the HFSS solver. Initially, a simulation of the nature-inspired FSS is conducted with a single layer, comprising a single spiral for both vertical and horizontal polarization.

The initial analysis involved varying the parameter a while setting k to 0.16, w to 0.3 mm, and P to 35 mm. The unit cells depicted in Fig. 3 were considered for different values of a .

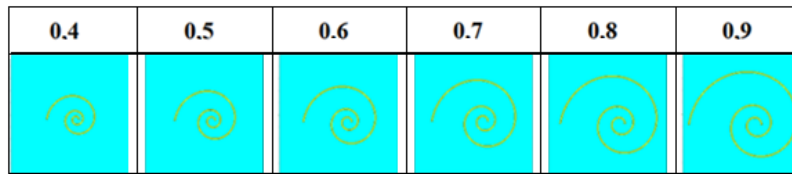


Fig. 3. Unit cells for a variation.

Increasing the variable a leads to a larger size of the FSS spiral, thereby increasing its inductance and causing a reduction in the resonance frequency, as illustrated in Fig. 4. When a is set to 0.4, there is no resonance below -10 dB within the frequency range of interest. As a is further increased, the resonance decreases. Specifically, for a equal to 0.5, the resonance occurs at 10.65 GHz, while for a equal to 0.7, it shifts to 8.05 GHz. Finally, with a set to 0.9, the resonance is observed at 6.25 GHz.

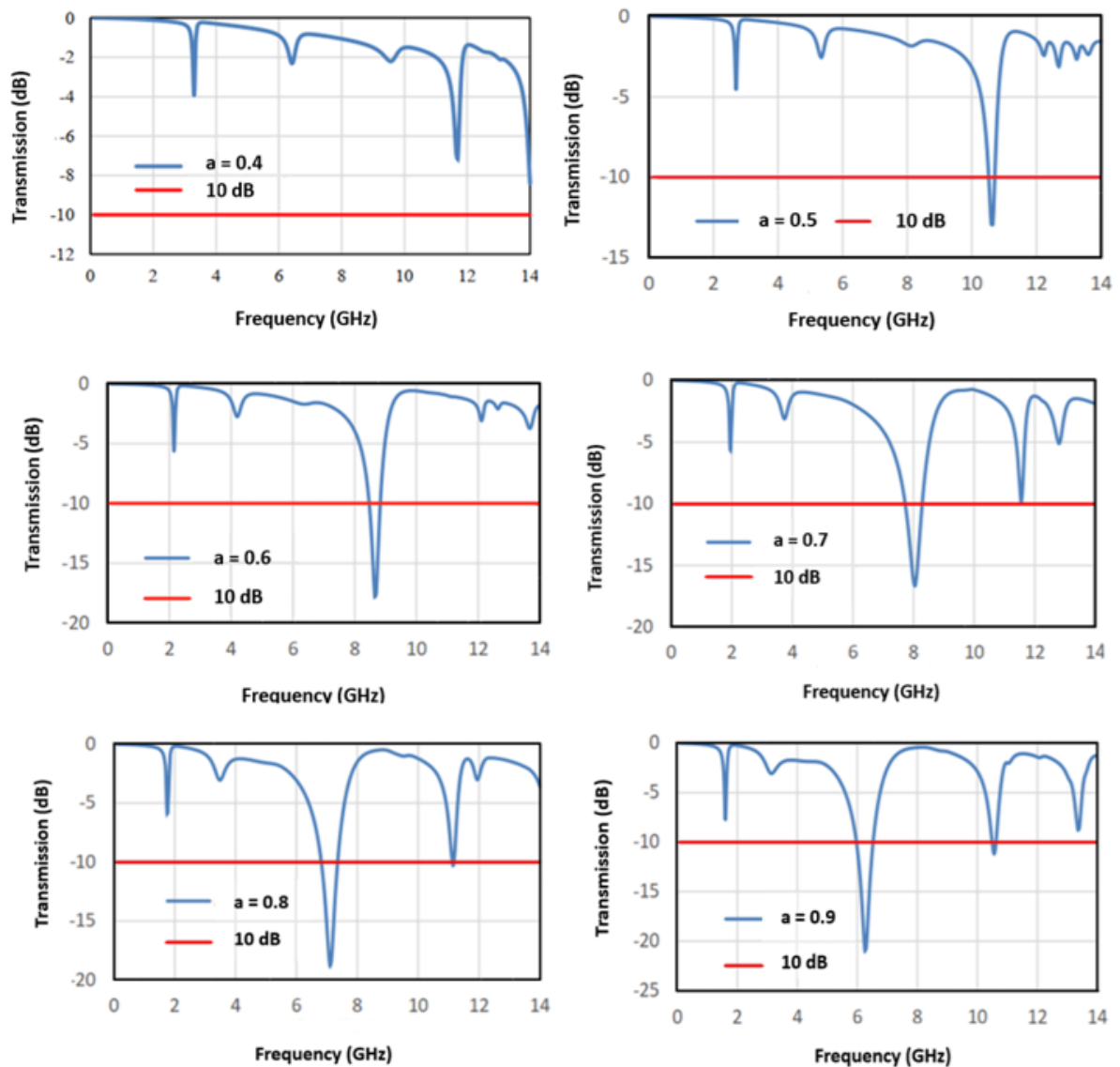


Fig. 4. Transmission coefficient in dB for different values of a .

The second analysis involved varying the parameter k while setting a to 0.9, w to 0.3 mm, and P to 35 mm. The unit cells depicted in Fig. 5 were considered for different values of k .

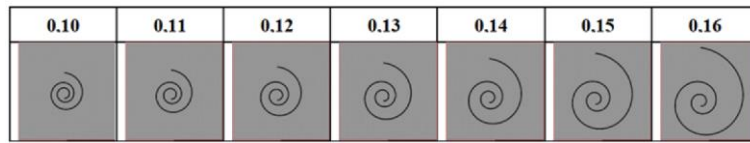


Fig. 5. Unit cells for k variation.

An increase in the variable k also results in an increase in the loop's inductance, thereby reducing the resonance frequency. For k values equal to 0.11, 0.12, and 0.13, FSS did not resonate frequencies below -10 dB within the analyzed range. Resonance occurred at 7.90 GHz for $k = 0.14$, at 7.05 GHz for $k = 0.15$, and at 6.20 GHz for $k = 0.16$, as illustrated in Fig. 6.

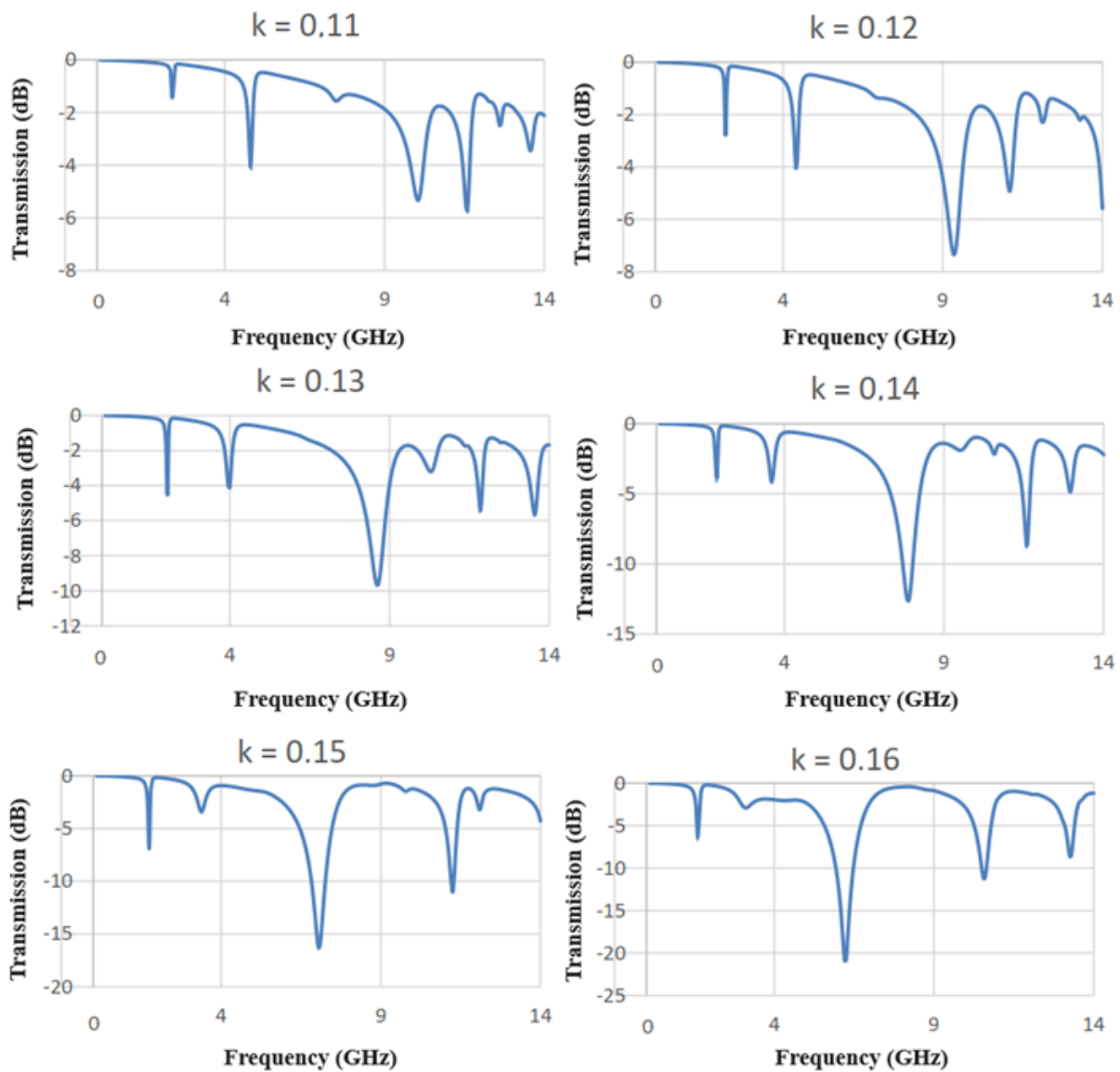


Fig. 6. Transmission coefficient in dB for different values of k .

The final analysis involved varying the parameter w while setting a to 0.9, k to 0.16 mm, and P to 35 mm. The unit cells illustrated were considered for different values of w in Fig. 7.

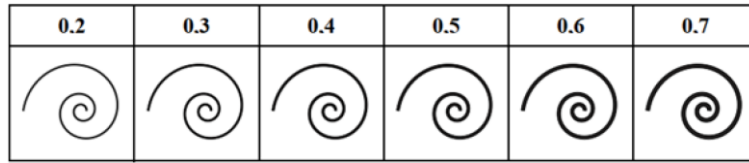


Fig. 7. Unit cells for w variation.

With the variation of the thickness of the spiral strip, w , it can be observed that as the thickness increases, there is an increase in the main resonance frequency, ranging from 6.2 to 6.6 GHz, for the w variations adopted. For $w = 0.2$ mm, the resonance frequency, f_r , was 6.2 GHz, while for $w = 0.5$ mm, f_r was 6.5 GHz. Finally, for $w = 0.7$ mm, f_r was 6.6 GHz. Additionally, it can be noted that there is the emergence of a second resonance frequency, which undergoes little change for different values of w . This can be seen in Fig. 8.

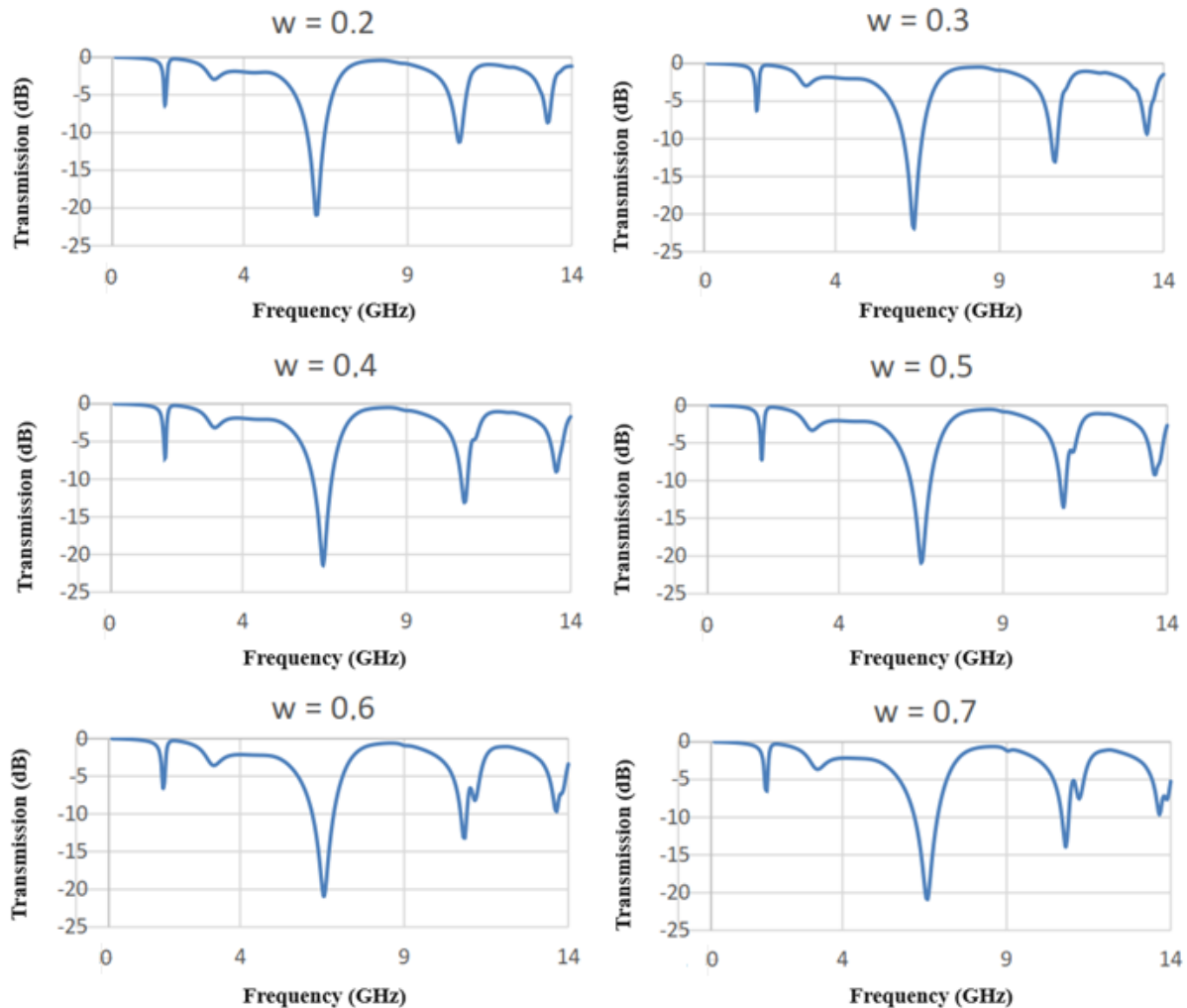


Fig. 8. Transmission coefficient in dB for different values of w .

IV. PROPOSED STRUCTURE

After the extensive parametric analysis, we chosen the values $a = 1.8$, $b = 0.165$, $k = 0.15$, and $w = 0.3$ mm. The simulation involves the spiral in its initial position (0°) and the same spiral rotated clockwise by 90° . The results are depicted in Fig. 9, 0° position (Fig. 9(a)) and, 90° position (Fig. 9(b)). Regarding the 0° position, for horizontal polarization (H pol.), one resonance is observed at 3.5 GHz with a bandwidth of 270 MHz (Fig. 8 (a)), while for vertical polarization (V pol.), two resonances are observed (Fig. 9 (a)). The first resonance occurs at 1.65 GHz with a bandwidth of 70 MHz, and the second resonance occurs at 2.45 GHz with a bandwidth of 200 MHz. When the spiral is rotated 90° clockwise (Fig. 9 (b)), the opposite behavior is observed. The horizontal polarization response exhibits two resonances: the first at 1.65 GHz with a bandwidth of 70 MHz, and the second at 2.45 GHz with a bandwidth of 200 MHz. Conversely, in vertical polarization, a single resonance is observed at 3.5 GHz with a bandwidth of 270 MHz.

The single-layer FSS (Fig. 2(a)) and the FSS rotated clockwise by 90° do not demonstrate polarization independence or angular stability, but they exhibit complementary responses. Therefore, we decided to cascade the two structures to achieve these characteristics. The proposed cascaded structure is depicted in Fig. 10(a) and Fig. 10(b). This structure consists of two layers with a distance of 18 mm between them. The cascaded structure displays a multiband frequency response. The transmission coefficient under normal incidence of the proposed cascaded FSS is illustrated in Fig. 11. The FSS provides stopband resonances at 1.63 GHz, 2.46 GHz, and 3.43 GHz.

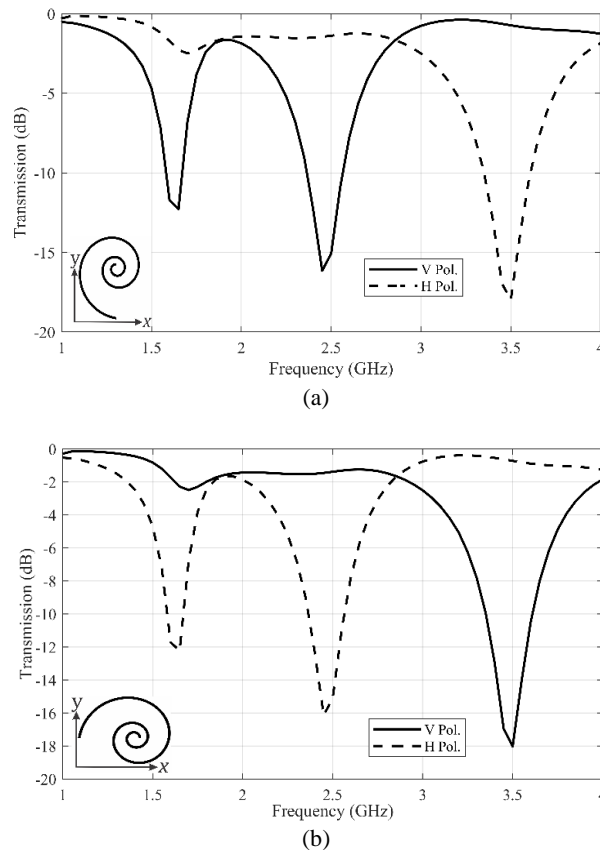
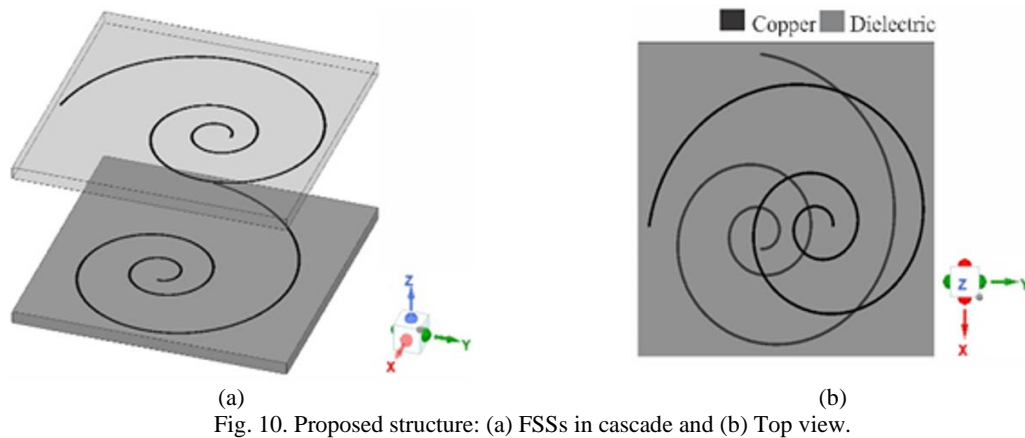


Fig. 9. Transmission frequency responses for normal incidence: (a) spirals in 0° and (b) spirals in 90° position.



(a) (b)
 Fig. 10. Proposed structure: (a) FSSs in cascade and (b) Top view.

Fig. 12(a) illustrates the electric field on the cascaded FSS for vertical polarization, while Fig. 12(b) illustrates the electric field on the cascaded FSS for horizontal polarization, both at 2.47 GHz and under normal incidence. It is evident that for vertical polarization, the field is more intense on the top FSS, whereas for horizontal polarization, the field is more intense on the bottom FSS. This observation justifies the complementary response of the two FSSs.

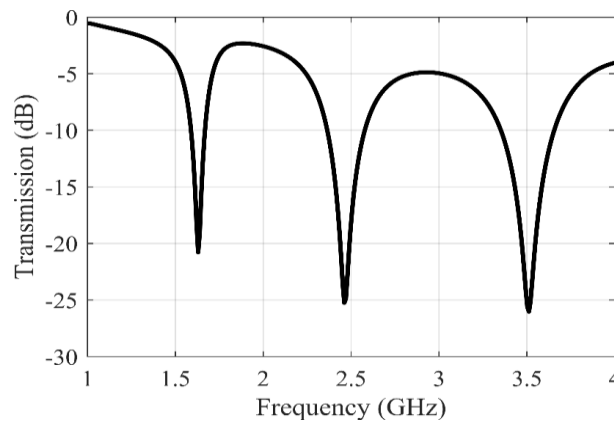
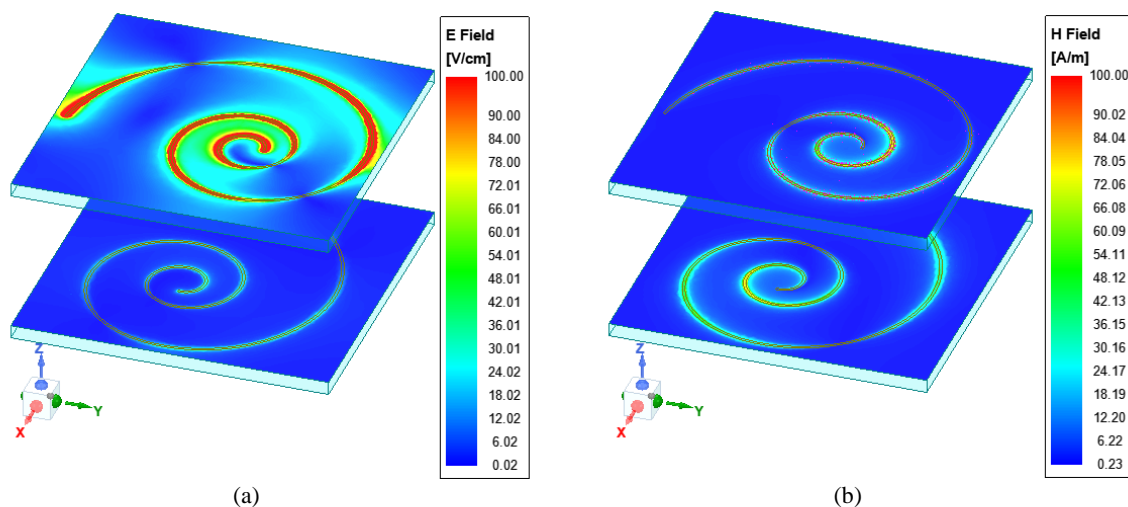


Fig. 11. Frequency response of cascaded FSSs.



(a) (b)
 Fig. 12. Electric field on the cascaded FSSs at 2.47 GHz: (a) vertical polarization and (b) horizontal polarization.

V. EXPERIMENTAL RESULTS

To validate the numerical results, prototypes of the two FSSs were constructed and cascaded. Images

of the fabricated samples are depicted in Fig. 13. The proposed structure was evaluated using the free-space method. The measurement setup comprised a vector network analyzer (VNA, Keysight model N5071C two ports networks analyzer [27]), two double ridge ultra-wideband horn antennas (model SAS-571 from A. H. Systems, with an operating range from 700 MHz to 18 GHz [28]), and a measurement window (see Fig. 14). The distance between the antennas is approximately 2.6 m, and the measurement window is positioned equidistantly from both antennas.



Fig. 13. Fabricated prototypes.

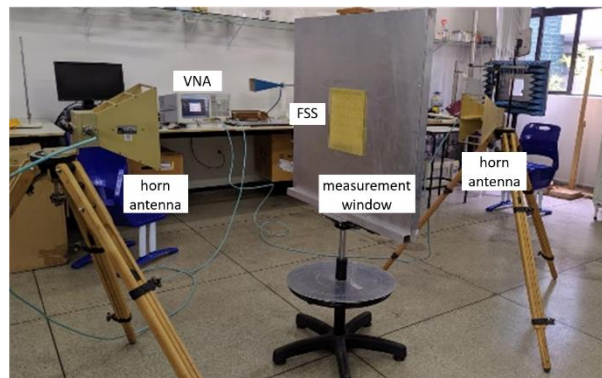


Fig. 14. Measurement setup.

The measurement of the spiral in the 0° position (Fig. 9(a)) was conducted for vertical polarization, electric field in y direction, normal incidence, and the comparison with simulation results is depicted in Fig. 15. According to the simulation, the first resonance occurs at 1.65 GHz, with the -10 dB stopband extending from 1.60 GHz to 1.67 GHz. The second resonance is observed at 2.45 GHz, with the -10 dB stopband spanning from 2.37 GHz to 2.57 GHz. Conversely, experimental findings indicate that the first resonance takes place at 1.70 GHz, with the -10 dB stopband spanning from 1.64 GHz to 1.71 GHz, while the second resonance occurs at 2.46 GHz, with the -10 dB stopband ranging from 2.35 GHz to 2.58 GHz. There is a good agreement between numerical and measured results.

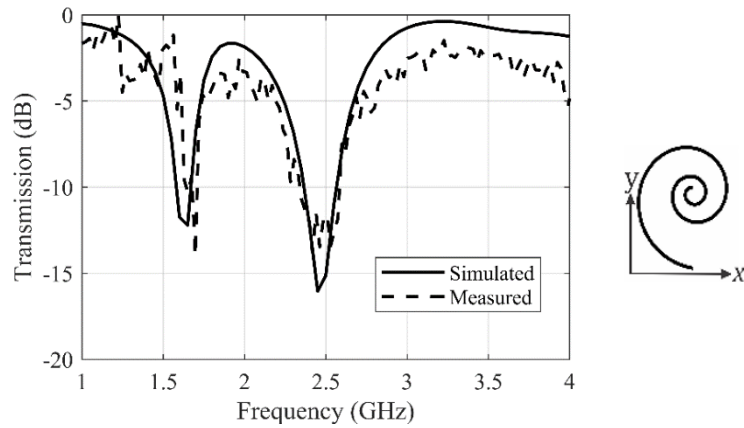


Fig. 15. Comparison between simulation and experimental results for the FSS, spiral in 0° position, normal incidence.

The second measurement involves rotating the spiral clockwise by 90 degrees, 90° position (Fig. 9(b)). Fig. 16 presents the comparison between simulation and experimental results. According to the simulation, there is a resonance at 3.50 GHz, with the -10 dB stopband spanning from 3.35 GHz to 3.62 GHz. Experimental results indicate a resonance at 3.50 GHz, with the -10 dB stopband extending from 3.36 GHz to 3.66 GHz. Once more, a good agreement between the results can be observed.

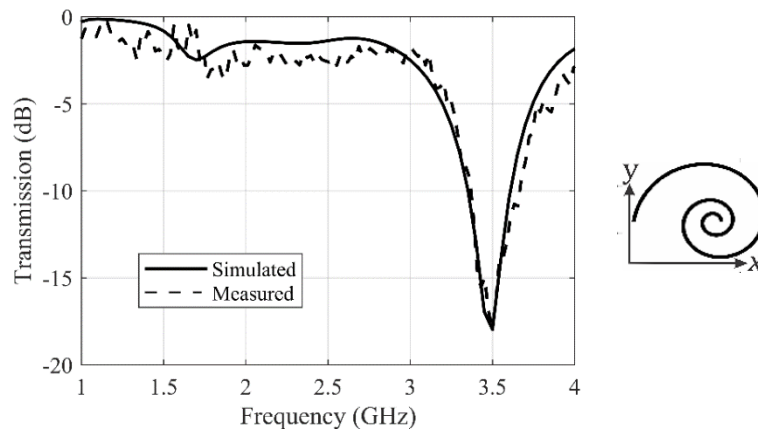


Fig. 16. Comparison between simulation and experimental results for the FSS, spiral in 90° position, normal incidence.

The third measurement utilizes the proposed structure, comprising two cascaded FSS elements separated by 18 mm of air. Fig. 17 illustrates the comparison between simulation and experimental results. According to the simulation, three resonances are observed: the first resonance at 1.63 GHz with a -10 dB stopband spanning from 1.59 GHz to 1.67 GHz, the second resonance at 2.46 GHz with a -10 dB stopband spanning from 2.36 GHz to 2.58 GHz, and the third resonance at 3.43 GHz with a -10 dB stopband spanning from 3.26 GHz to 3.69 GHz.

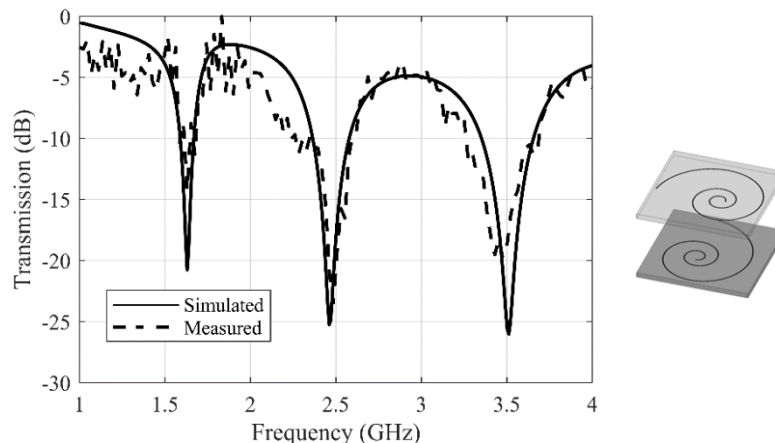


Fig. 17. Comparison between simulation and experimental results of the proposed structure, normal incidence.

Finally, measurements of horizontal and vertical polarizations with oblique incidence up to 45 degrees are shown in Fig. 18 (a) and Fig 18 (b), respectively. It is evident that the bandwidth does not suffer degradation in both polarization cases, thus confirming angular stability and polarization independence.

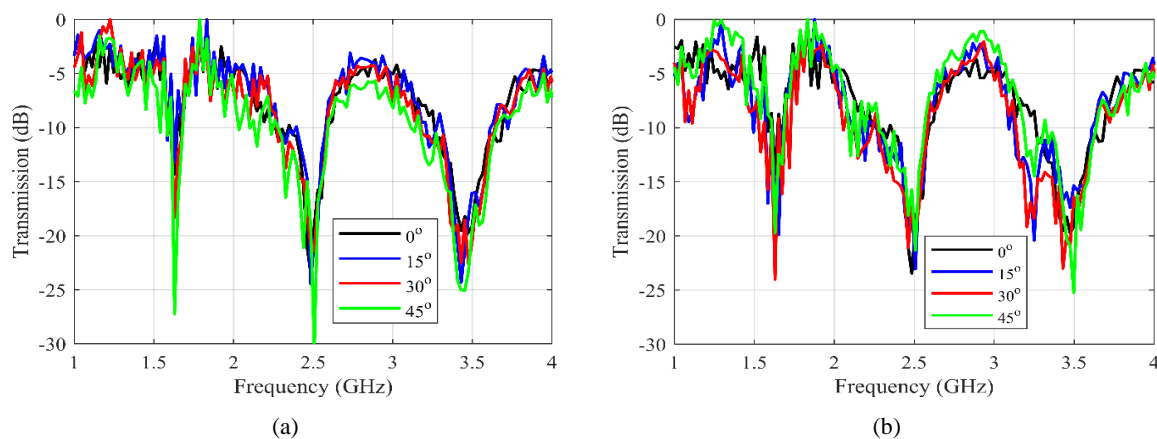


Fig. 18. Experimental results with oblique incidence up to 45°: (a) Horizontal polarization and (b) Vertical polarization.

VI. CONCLUSIONS

In this paper, we introduce a nature-inspired tri-band FSS with closely spaced resonant frequencies ($FR < 2$). By cascading two identical nature-inspired geometries, we achieved an FSS exhibiting a tri-band response with closely resonant bands, angular stability, and polarization independence. The FR from the second to the first resonant frequencies is 1.48, and the FR from the third to the second resonant frequencies is 1.43. The proposed FSS is suitable for applications in ISM (2.40 to 2.4835 GHz) and 5G NR bands (3.3 to 3.7 GHz). The nature-inspired cascaded FSS structure ensures angular stability and polarization independence while remaining a low-cost and easy-to-fabricate solution. Strong agreement between simulation and experimental results has been observed, with errors less than 1% for resonance frequencies and bandwidths. This indicates the potential of the proposed structure for various modern communication systems. In future research, we plan to conduct an extensive parametric investigation covering all parameters, including r , a , b , w , θ , and P . This investigation aims to provide comprehensive

insights into various aspects, such as the angular stability influenced by the Fibonacci spiral geometry and the impact of polarization on the structure's performance.

REFERENCES

- [1] B. A. Munk, *Frequency Selective Surfaces – Theory and Design*, New York: John Wiley and Sons, Inc., 2000.
- [2] M. Li, L. Zhou and Z. Shen, “Frequency Selective Radome with Wide Diffusive Bands”, *IEEE Antennas and Wireless Propagation Letters*, vol. 21, no. 2, pp. 327 – 331, 2022.
- [3] F. Costa, S. Genovesi, A. Monorchio and G. Manara, “A Robust Differential-Amplitude Codification for Chipless RFID”, *IEEE Microwave and Wireless Components Letters*, vol. 25, no. 12, pp. 832 – 834, 2015.
- [4] D. S. Escuderos, H. C. M. Li, E. A. Daviu, M. C. Fabr s and M. F. Bataller, “Microwave Planar Lens Antenna Designed with a Three-Layer Frequency-Selective Surface”, *IEEE Antennas and Wireless Propagation Letters*, vol. 16, pp. 904 – 907, 2017.
- [5] D. Li, T. W. Li, E. P. Li and Y. J. Zhang, “A 2.5-D Angularly Stable Frequency Selective Surface Using Via-Based Structure for 5G EMI Shielding”, *IEEE Transactions on Electromagnetic Compatibility*, vol. 60, no. 3, pp. 768 – 775, 2018.
- [6] M. A. Al-Joumayly and N. Behdad, “Low-Profile, Highly-Selective, Dual-Band Frequency Selective Surfaces with Closely Spaced Bands of Operation”, *IEEE Transactions on Antennas and Propagation*, vol. 58, no. 12, 4042 – 4050, 2010.
- [7] A. L. P. S. Campos, R. H. C. Mani oba, L. M. Ara jo and A. G. d’Assun o, “Analysis of Simple FSS Cascading with Dual Band Response”, *IEEE Transactions on Magnetics*, vol. 46, no. 8, pp. 3345 – 3348, 2010.
- [8] Y. Y. Lv and W. L. Chen, “Dual-Polarized Multiband Frequency Selective Surface with Miniaturized Hilbert Element”, *Microwave and Optical Technology Letters*, vol. 55, no. 6, pp. 1221 – 1223, 2013.
- [9] B. S. Izquierdo, E. Parker, J. B. Robertson and J. C. Batchelor, “Single and Dual Polarized Convolutional Frequency Selective Structures”, *IEEE Transactions on Antennas and Propagation*, vol. 58, no. 3, pp. 690 – 696, 2010.
- [10] L. Mingyun, H. Minjie, and W. Zue, “Design of multi-band frequency selective surfaces using multi-periodicity combined elements”, *Journal of Systems Engineering and Electronics*, vol. 20, no. 4, p. 675–680, 2009.
- [11] D. H. Kim and J. I. Choi, “Design of a Multiband Frequency Selective Surface”, *ETRI Journal*, vol. 28, no. 4, pp. 506 – 508, 2006.
- [12] B. Bhushan, *Biomimetics: bioinspired hierarchical-structured surfaces for green science and technology*, Berlin, Germany: Springer, 2012.
- [13] S. Vajda, *Fibonacci and Lucas numbers, and the golden section: theory and applications*, New York, NY: Halsted Press, 1989.
- [14] M. Livio, *The golden ratio: the story of phi, the world’s most astonishing number*, New York, NY: Broadway Books, 2002.
- [15] A. Posamentier and I. Lehmann, *The fabulous Fibonacci numbers*, New York, NY: Prometheus Books, 2007.
- [16] G. Bixler and B. Bhushan, “Fluid drag reduction and efficient self-cleaning with rice leaf and butterfly wing bioinspired surfaces”, *Nanoscale*, no. 5, pp. 7685 – 7710, 2013.
- [17] M. D. S. Mesquita, A. G. d’Assun o, J. B. L. Oliveira, and Y. M. V. Batista, “A New Conductive Ink for Microstrip Antenna and Bioinspired FSS Designs on Glass and Fiberglass Substrates”, *Journal of Microwaves, Optoelectronics and Electromagnetic Applications*, vol. 18, no. 2, pp. 227 – 243, 2019-245.
- [18] V. k. Kanth and S. Raghavan, “Hybrid Complementary FSS Element based on Fibonacci Spiral for Triple-band EMI Shielding Application”, *2019 IEEE 5th Global Electromagnetic Compatibility Conference (GEMCCON)*, Bangalore, India, pp. 1 – 4, 2019.
- [19] K. Varikintla and R. Singaravelu, “Design of a novel 2.5D frequency selective surface element using Fibonacci spiral for radome application”, *2018 Asia-Pacific Microwave Conference (APMC)*, Kyoto, pp. 1289 – 1291, 2018.
- [20] M. S. Kelley and G. H. Huff, “Fluidic Tuning of a Frequency Selective Surface based on a Four-Arm Archimedean Spiral”, *2013 IEEE Antennas and Propagation Society International Symposium (APSURSI)*, Orlando, FL, pp. 468 – 469, 2013.
- [21] M. Kelley and G. Huff, “Dual-band frequency selective surfaces based on multi-arm sub-wavelength Archimedean spirals”, *Electronics Letters*, vol. 51, no. 19, pp. 1476 – 1478, 2015.
- [22] D. K. Wickenden, R. Awadallah, P. A. Vichot, B. M. Brawley, *et al*, “Polarization Properties of Frequency-Selective Surfaces Comprised of Spiral Resonators”, *IEEE Transactions on Antennas and Propagation*, vol. 55, no. 9, pp. 2591 – 2597, 2007.
- [23] The fibonacci sequence in nature, Available at <https://spectramagazine.org/mathematics/the-fibonacci-sequence-in-nature/>, accessed in 14th, June of 2023.
- [24] R. C. Yates, *A Handbook on Curves and their Properties*, USA: Digital reprint by www.CircuitousRoot.com, 1947.
- [25] E. H. Lockwood, *Book of Curves*, Cambridge: Cambridge University Press, 1961.
- [26] D. J. Darling, *The universal book of mathematics: from Abracadabra to Zeno’s paradoxes*, John Wiley and Sons. p. 188, 2004.
- [27] Analisador de rede vetorial ENA E5071C, Available at <https://www.keysight.com/br/pt/product/E5071C/e5071c-ena-vector-network-analyzer.html>, accessed in 14th, June of 2023.
- [28] Double Ridge Guide Horn Antenna, Available at <https://www.ahsystems.com/catalog/SAS-571.php>, accessed in 14th, June of 2023.